THE STATE OF THE ART IN ASSESSING STRUCTURAL INTEGRITY

I. Milne*

Four methods of asessing the integrity of a cracked structure are reviewed, concentrating on the practical requirements of the various methods such as the use of stress strain data, and the treatment of materials toughness and thermal stresses. Some of the difficulties and approximations identified by recent EGF predictive exercises are discussed. Particular emphasisis addressed to the way the methods have been validated, and whether they are capable of providing consistent solutions, which are user insensitive. The advantages and disadvantages of each of the methods are summarised.

INTRODUCTION

The facility to evaluate the defect tolerance of a structure has a number of advantages. At the design stage it may be used to optimise the design with respect to material properties, inspectability and geometric details. During operation it may be used to reassess plant which have been found to contain defects, provide a facility to extend the lifespan of plant, uprate (or otherwise modify) plant operating conditions, enable the planning of outages for inspection or refurbishment, and provide the basis for an efficient inspection strategy. Both during design and operation, the same objectives apply, i.e. the optimisation of safety, reliability, efficiency and cost effectiveness.

The role of fracture mechanics in establishing structural integrity is now well established and used by all high technology industries. Techniques

* Central Electricity Research Laboratories, Kelvin Avenue, Leatherhead, Surrey, UK.

are often developed and applied extemporaneously, using for example modern concepts of J* based upon the theories and developments of Rice (1) and Hutchinson and Paris (2) and using finite element methods or complex analytical methods to perform the calculations. Such methods are, however, often expensive, difficult to validate and are not amenable to ready application and assessment by independent authorities. Hence a number of standardised procedures have been developed, the most successful of which should have the following attributes:

1. they are relatively simple, having standardised rules to favour consistent application.

2. they can handle a large number of variables efficiently and cheaply, such as crack sizes and shapes, locations, loading states, material properties.

3. they can handle special circumstances well, where necessary by resorting to empirical solutions.

4. they have been validated on relevant structural geometries and are accepted by authoritative bodies as such.

In this paper attention will be focussed on four of the most widely used methods, addressing in particular the way they treat specific features of the analysis and the quality of their validation.

METHODS

The four methods selected may be thought of as being sufficiently well documented to be generally applicable by non-authors. In order of historical development they are

the crack opening displacement (COD) method

the R6 method

the GE scheme

and the engineering J design curve (EnJ).

The first two of these are designed to be total packages, documented as step-wise procedures whose end product

* Footnote. To save space parameters are not defined in the text. A list of definitions appears at the end of the paper.

TABLE 1 - Equations in form used by various methods

Method	Equations	Comment
GE	$J = \frac{K^2(a_e)}{E'} + \alpha\varepsilon_0\sigma_0 c\, h_1(n, a/t)(P/P_0)^{n+1}$ $a_e = \frac{1}{\beta\pi}\frac{n-1}{n+1}\left(\frac{K}{\sigma_0}\right)^2\frac{1}{1+(P/P_0)^2}$; $c = t-a$ $E' = E$ or $E/(1-\nu^2)$	$\sigma_0, \varepsilon_0, \alpha, n$ from Ramberg Osgood law of true stress-true strain curve. P_0, h_1 given in (7,8) $\beta = 2$ in plane stress, 6 in plane strain K evaluated for $\sigma^P + \sigma^S$ stresses.
EnJ	$\frac{J}{G\gamma} = \left(\frac{\varepsilon_f}{\varepsilon_y}\right)^2\left\{1 + 0{\cdot}5\left(\frac{\varepsilon_f}{\varepsilon_y}\right)^2\right\}$; $\sigma/\sigma_y \leqslant 1{\cdot}2$ $\frac{J}{G\gamma} = 2{\cdot}5\left\{\frac{\varepsilon_f}{\varepsilon_y} - 0{\cdot}2\right\}$; $\sigma/\sigma_y \geqslant 1{\cdot}2$	ε_f -effective strain (10), $cbs\varepsilon$. $\frac{cbs\varepsilon}{\varepsilon_y, \alpha} = h_g\left\{\frac{cbs\sigma}{\sigma_y}(1+\alpha) - (\beta_t + \beta_b)\right\}$ g, α - geometric terms, h - hardening term, β_t, β_b - tensile, bending terms (see (10)).
R6 Rev.3	$K_r = \left\{\frac{E\varepsilon_{ref}}{L_r\sigma_y} + \frac{L_r^3\sigma_y}{2E\sigma_{ref}}\right\}^{-1/2}$; $L_r \leqslant L_r^{max}$ $K_r = 0$; $L_r > L_r^{max}$, $L_r^{max} = \sigma_{flow}/\sigma_y$	$\sigma_{ref}, \varepsilon_{ref}$ from true stress true strain curve, $L_r\sigma_y = \sigma_{ref}$ Analysis by use of failure assessment diagram
COD 1	$\frac{\delta_{crit}E}{2\pi\sigma_y a} = \left\{\frac{\sigma^P + \sigma^S}{\sigma_y}\right\}^2$; $\sigma^P + \sigma^S < 0{\cdot}5\sigma_y$ $\frac{\delta_{crit}E}{2\pi\sigma_y a} = \left\{\frac{\sigma^P + \sigma^S}{\sigma_y} - 0{\cdot}25\right\}$; $\sigma^P + \sigma^S > 0{\cdot}5\sigma_y$	$\sigma^P = K^P/\sqrt{\pi a}$; $\sigma^S = K^S/\sqrt{\pi a}$ δ crit - COD measured from full section thickness test. Use only when $\sigma_n < 0{\cdot}85\,\sigma_y$ (equivalent to $L_r < 0.85$)
COD 2	$\frac{\delta E}{\pi\sigma_y a} = \left\{\frac{\sigma^P}{\sigma_y}\left[\frac{8}{\pi^2}\ln\sec\frac{\pi}{2}\frac{\sigma_n}{\sigma_y}\right]^{1/2} + \frac{\sigma^S}{\sigma_y}\right\}^2$	σ_n - net section stress, as used for COD 1
COD 3	$\frac{\delta E}{\pi\sigma_y a} = \left\{\frac{\sigma^P}{\sigma_y}\left[\frac{2a_e}{a}\right] + \frac{E\varepsilon_{ref}}{\sigma_{ref}} - 1\right]^{1/2} + \frac{\sigma^S}{\sigma_y}\right\}^2$ $a_e = a + \frac{1}{2\pi}\left(\frac{K^P}{\sigma_y}\right)^2\frac{1}{1+\sigma_{ref}/\sigma_y}$	$\sigma_{ref}, \varepsilon_{ref}$ as for R6 Rev. 3

is an estimate of the relative integrity of a structure. Careful consideration has been given to the required material properties, which have been tailored to the requirements of the techniques. Both techniques have undergone revision since they were first published, and the following discussion will be based on the most modern revisions or proposals which are generally available at the time of writing. These are revision 3 of R6, termed R6 Rev. 3 (3,4) and the proposed 3-tier COD techniques (5), termed respectively COD 1, COD 2 and COD 3.

The third and fourth methods aim to provide estimates of the J applied to a structure, and the user has to decide how to use this parameter and what material properties are appropriate for its use. Guidance is, of course, given, but this is only in a general sense. The GE scheme (6) is documented in EPRI publications (7,8) while details of EnJ (9) may be obtained from publications of the Ispra courses (10).

The GE scheme stands apart from the other 3 methods in claiming to provide an explicit evaluation of J rather than an approximation. An advantage of this is that there exists a rigorous link between the GE J estimates and J obtained by finite element methods. Attendant disadvantages are that at present only a limited number of simple 2-dimensional problems may be analysed and there is no facility to broaden the method to incorporate empirical solutions. This limitation can be overcome by replotting the GE-J values on R6 axes (11). This technique will not be addressed specifically here as it is really a special case of the GE or R6 methods. Similarly the J-T diagram (12) will not be considered as this is only a special case of J analysis used to define ductile instability. After the instability point has been defined the load and defect tolerance must still be evaluated by a separate J analysis.

EQUATIONS

Table 1 lists the equations utilised in the different techniques along with the necessary comment and definitions. These equations effectively define the applied loading parameter (J, COD or K equivalent) as a function of the load (or equivalent strain) applied in the form appropriate for their specific use. Thus for R6 Rev. 3 the equation defines the failure assessment diagram (FAD) which is used to perform the

TABLE 2 - Comparison of normalised equations

Method	Normalised Equations (σ^p stresses only)
GE	$\frac{J}{G_y} = \left(\frac{\sigma^p}{\sigma_y}\right)^2 \frac{a_e}{a} + \frac{\alpha \sigma_o c h_1}{\sigma_y^2 y^2 a}\left(\frac{P}{P_o}\right)^{n+1}$ $= \left(\frac{\sigma^p}{\sigma_y}\right)^2 \left\{\frac{a_e}{a} + \alpha\left(\frac{t}{a} - 1\right)\frac{h_1}{y^2}\left(\frac{P}{P_o}\right)^{n-1}\right\}$ for $\sigma_y = \sigma_o = E'\varepsilon_o$
R6 Rev. 3	$\frac{J}{G_y} = \left(\frac{\sigma^p}{\sigma_y}\right)^2 \left\{\frac{L_r^3 \sigma_y}{2E\varepsilon_{ref}} + \frac{E\varepsilon_{ref}}{\sigma_{ref}}\right\}$; $L_r < \frac{\sigma_{ref}}{\sigma_y}$
COD 3	$\frac{J}{G_y} = m\left(\frac{\sigma^p}{\sigma_y}\right)^2 \left\{\frac{a_e}{a} - 1 + \frac{E\varepsilon_{ref}}{\sigma_{ref}}\right\}$
COD 2	$\frac{J}{G_y} = m\left(\frac{\sigma^p}{\sigma_y}\right)^2 \left\{\frac{1}{L_r}\left[\frac{8}{\pi^2} L_r \sec\left(\frac{\pi}{2} L_r\right)\right]^{1/2}\right\}^2$
COD 1	$\frac{J}{G_y} = 2m\left(\frac{\sigma^p}{\sigma_y}\right)^2$; $\sigma_{nominal} \lesssim 0.5$ $\frac{J}{G_y} = 2m\left\{\frac{\sigma^p}{\sigma_y} - 0.25\right\}$; $\sigma_{nominal} \lesssim 0.5$, $L_r < 0.8$
EnJ	$\frac{J}{G_y} = \left(\frac{\sigma^p}{\sigma_y}\right)^2 \left\{1 + 0.5\left(\frac{\sigma^p}{\sigma_y}\right)^2\right\}$; $\sigma_{nom} \lesssim 1.2$, $\frac{\sigma^p}{\sigma_y} = \frac{\varepsilon_f}{\varepsilon_y}$ $\frac{J}{G_y} = 2.5\left\{\frac{\varepsilon_f}{\varepsilon_y} - 0.2\right\}$; $\sigma_{nom} > 1.2$

analysis while for the GE scheme the equation simply defines the J applied to the structure.

A direct comparison of these equations can be made by normalising them appropriately, say by G_y, the elastic energy release rate at an applied stress equal to the yield stress. Taking $J = m\sigma_y\delta$ (where δ is the applied COD and m is a factor which depends upon geometry, state of strain and strain hardening index) removing the thermal and residual (σ^s) component from the COD equations, and recognising that $\sigma_n/\sigma_y = L_r$, the equations in Table 2 are obtained. These divide into two basic groups, the first containing COD 1 and EnJ, the second containing the GE scheme, R6 Rev. 3 and COD 3. COD 2 may be considered to be a special case of COD 3 where the benefit of strain hardening has been removed.

Taking the second of these groupings first, there is a clear similarity between COD 3 and R6 Rev. 3, where reference stress techniques are used to derive the strain hardening characteristics in applied J. The reference stress technique was developed by Ainsworth (13) to overcome the deficiencies inherent in the GE scheme obtained by relying on a Ramberg-Osgood power law fit to the material's stress strain curve (14). However, Ainsworth's equation was derived from the GE scheme, and uses the same technique of dividing the J applied into two terms, a first order plastic term and a fully plastic term. These are respectively the first and second terms in the GE equations in Table 2, and they may be compared with the first and second terms in the R6 Rev. 3 equations in that Table. Both equations give similar results when the stress strain data may be properly represented by a Ramberg Osgood law (15), but the R6 Rev. 3 equation gives the better result for other situations (16). COD 3 (Table 2) uses the R6 Rev. 3 fully plastic term and the GE first order plastic term slightly modified (Table 1). Thus, apart from minor differences in the definition of their principle components the GE scheme R6 Rev. 3 and COD 3 equations may be considered to be similar.

COD 2 owes its parentage to the original form of R6, with the plastic collapse term, S_r (17) replaced by the plastic yield term, L_r. While there is no direct mathematical link to the other 3 equations contained in this group, it follows a similar form to these 3 equations at net section stresses below yield.

In the first group of equations there is also a similarity, but this does not arise from any common link. COD 1 is essentially a restatement in terms of applied stresses, of the empirically based COD design curve developed by Burdekin and Dawes (18) while EnJ was derived as an upper bound curve to J estimates of a number of geometries obtained using finite element methods. The similarities are therefore fortuitous. The differences become more apparent in application when the EnJ term $\varepsilon_f/\varepsilon_y$ exceeds σ/σ_y, i.e. at high stress levels where COD 1 is stated to be inapplicable. In this regime the EnJ equation is intended to provide an allowance for displacement control, where appropriate (9).

INPUT

Treatment of Tensile Data

Both COD 1 and COD 2 are defined solely in terms of the yield stress, σ_y, and make no allowance for the extra load carrying capacity obtained by work hardening. In this respect their use is unambiguous. The same cannot be said of the GE scheme or EnJ, where strain hardening effects are incorporated by the use of a power law equation.

In the GE scheme this is the Ramberg Osgood (RO) law, expressed in terms of the normalised values of stress and strain, σ/σ_o and $\varepsilon/\varepsilon_o$, where σ_o and ε_o are reference values of stress and strain, and the parameters α and n, as

$$\frac{\varepsilon}{\varepsilon_o} = \frac{\sigma}{\sigma_o} + \alpha\left(\frac{\sigma}{\sigma_o}\right)^n$$

The terms α and n have a strong influence on the fully plastic term in the GE equation (Table 1) and need to be chosen with care. Unfortunately, there is no guidance given as to how best to fit the R.O. equation to the material's data, and while this is seldom significant when dealing with materials with a low strain hardening capacity it creates major problems for other materials, especially austenitic and carbon manganese steels (14). This difficulty was highlighted in the first phase of the recent EGF round robin exercise in predicting ductile instability (19) where participants attempted a blind prediction of the load - crack extension behaviour of two compact tension test pieces. The material was A533B steel and tensile data was tabulated as true stress-true

strain data. Wide variations of R.O. parameters were obtained with extremes in α of 0.9 and 6.31 and in n of 6.07 and 10.8. The data is plotted out on Fig. 1 and compared with two of the best fits obtained. Fit 1 appeared to be chosen to smooth out the lower yield strain at the expense of the high strain region while fit 2 ignored the lower yield strain to provide a good fit at high strains.

In EnJ strain hardening effects are incorporated by a (non-specified) power law, via a strain hardening index N where for low hardening $N \rightarrow o$ and for high hardening $N \rightarrow 1$ (10). The allowance is made in the calculation of the term $\varepsilon_f / \varepsilon_y$ (Table 1) using the concept of "cracked body structural strain", $_{cbs}\varepsilon$, via the multiplying factor h, where $h = 1/(N+1)$. So, as for the GE scheme, the final result depends sensitively on the way the tensile data is represented by the power law.

The inappropriate power law representation of tensile data (14) prompted the development of the reference stress technique (13), the basis of both R6 Rev. 3 and COD 3. In this technique the stress strain data is incorporated as co-ordinate points, ε_{ref}, σ_{ref}; obtained directly from the material's true stress-true strain curve. There is therefore no ambiguity in the use of this data and all fine detail may be represented accurately. This is important not only for austenitic steels but also for steels which exhibit an extensive lower yield plateau. In extreme cases, where the tensile component is sufficiently dominant the lower yield plateau can be obtained even in a cracked structure, as has been observed by Marandet et al (20). In these cases, power laws, being incapable of adequately representing the tensile data can only produce nonrepresentative estimates of J. Hence in applying the GE scheme to the test of Marandet et al (20) Rousselier obtained bad agreement between the test results and the GE predictions (21).

Of course, the requirement to accurately represent tensile data assumes that such data is always available. While this is generally true for modern plant it is seldom so for older plant and it may not be possible to extract specimens for tests. In cases like this R6 Rev. 3 contains an optional equation which is biased towards the lower bound of a number of curves obtained using the R6 Rev. 3 equation in Table 1 (4). Alternatively the equation can be limited to values of $L_r < 1$, where no advantage is taken of

the strain hardening effects. The result would be similar to that obtained using COD 2. EnJ may also be limited in this way but the GE scheme would have to be restricted to the first order plastic term. This would need to be modified to remove the dependence on n (Table 1) as indeed would a limited COD 3 equation.

Geometric effects

These are incorporated in the GE scheme in the first order plastic term through K and in the fully plastic term through the H functions and the reference load, P_o. The h functions are particularly useful, since these may be defined under load or displacement control thus allowing assessment of structures loaded under fixed displacement. This asset is unique to the GE scheme, although there is some allowance for displacement control in the EnJ method. In this case, however, the calculation is not straightforward, relying as it does on evaluating $\varepsilon_f/\varepsilon_y$ (Table 1). Modifications may also be made to R6 to cater for displacement control but this is not part of the standard procedure.

The GE scheme is restricted to 2-dimensional or axi-symmetric problems, while the other procedures are more generally applicable. In these other techniques the geometric effects are incorporated implicitly in the equations in Table 1, by the use of normalised parameters, with specific allowance made via the calculation of K and the plastic limit loads, where appropriate. The latter calculation is an integral part of R6 Rev. 3 and COD 2 and is a required but separate component in EnJ. It was shown to be a necessary adjunct to any analysis in phase I of the EGF exercise (19). In one case an inappropriate combination of estimates of J applied and J resistance parameters produced a high overestimate of the load capacity of a compact tension specimen which would not have occurred had plastic collapse been checked for explicitly.

Phase II of the EGF predictive exercise addressed the problem of a pressure vessel containing an axial semi elliptical surface defect (22). One participant applied the GE scheme, noting that the GE model assumed for the crack was a fully extended defect, and expecting a rather pessimistic result. The level of pessimism was large at initiation the prediction being 75% lower than the measured value, but the underestimate had decreased to 25% at the failure

pressure. This was because failure was dominated by plasticity of the ligament where the crack geometry had only a weak effect. It should not be assumed,however, that the GE scheme is always pessimistic when applied to defects of a finite length. In the presence of severe stress gradients, due possibly to thermal or residual stresses, or discontinuity stresses, cracks may propagate preferentially along the surface, as indicated in Fig. 2. The significance of this type of event can only be evaluated by addressing the deep point and the surface point on the crack front independently (4). This can be done using any of the COD techniques, R6 Rev. 3 or EnJ, and it may even be done using Bloom's representation of the GE scheme (11) provided that the normalisation on to the failure assessment diagram is accepted as applicable.

Neglecting the special geometric effect caused by fixed displacement loading, geometric dependance of normalised curves are of secondary importance compared with those due to the material's tensile properties. This is why the normalised procedures are so successful. The normalisation has, of course, to be done correctly and consistently, and it must be demonstrated to be valid by comparison with other techniques and test results. The normalisation used by Bloom (11) is based upon the reference load, P_o, of the GE scheme. This is not necessarily equivalent to the yield load and it also depends upon the choice of σ_o which is not necessarily the yield stress. These factors influence the h functions and hence the J applied. In plotting FADs obtained from the GE scheme, Bloom obtained a family of curves which showed a systematic dependence on crack size (11). This question was addressed specifically by Akhurst and Milne (16) and their experimental data showed no such dependence in the specimen geometries they tested. Confirmation of this was obtained in a recent 3-dimensional finite element analysis of cracked cylinders by the Lorenzi (8). It is likely that the crack size dependence obtained by Bloom is a feature of the 2-dimensional analysis used to derive the components of the GE scheme.

In Fig. 3 the experimental results from the 10 mm thick compact tension specimen used in the EGF phase 1 round robin exercise (19) are plotted in normalised units of J/G_y versus L_r. Superimposed on this are plots obtained using the GE scheme and

EnJ, and using R6 Rev. 3 and COD 3 (normalised by m and plotted at high values of L_r only). The R6 Rev. 3 cut-off at L_r^{max} has also been imposed on EnJ as this is equivalent to a specific plastic collapse condition. This Fig. shows that the reference stress techniques provide a better representation of the specimen behaviour than the techniques based on power laws.

All techniques provide similar estimates at $L_r<1$ (i.e. below net section yield). However, above this value of L_r EnJ follows a different form than the others. This arises from the attempt in EnJ to allow for displacement control. The real effect of this is somewhat obscure in Fig. 3, and is better depicted by plotting on R6 axes, as shown in Fig. 4, noting that at values of $L_r>1$ the EnJ L_r axis equates to $\varepsilon_f/\varepsilon_y$, not to σ/σ_y. When plotted in this way, it is apparent that the EnJ equations imply an inate level of stability at $L_r>1$, by virtue of the rising curve. The exact details of this cannot be inferred from this plot, however, since it depends upon the detailed calculation of the parameter cbsε in $\varepsilon_f/\varepsilon_y$.

Finally, to demonstrate the importance of correctly allowing for the detail of the stress strain curve, Fig. 5 shows some tensile data obtained from a carbon-manganese structural steel and Fig. 6 the R6 Rev. 3 FAD (Table 1). The vertical drop at $L_r=1$ is caused by the lower yield plateau in Fig. 5. Also included in Fig. 6 are data obtained from centre cracked panel test specimens of the carbon manganese steel (23), and a failure assessment line obtained from a specific finite element J solution obtained from a stress strain curve smoothed through the lower yield plateau. It is clear that only the reference stress technique provides a reasonable description of the experimental data.

Use of Toughness Data

Phase 1 of the EGF predictive exercise highlighted the need for adequate definitions of fracture toughness parameters. In the absence of adequate national standards unambiguous working definitions need to be incorporated into the procedures in order to avoid user-to-user variations. Although some guidance is given in the GE scheme and EnJ proposals about the use of toughness data, the problem of identifying

the required parameters has not been recognised.

The originally proposed COD technique, as used in BSI PD 6493(24) was designed around the use of 3 point bend COD specimens equal in thickness to the structure. The minimum of 3 test results is used in the analysis and, with the factors of safety contained in the COD design line this has been shown to provide a 97% confidence level that failure will be avoided (25). This level of confidence is presumably obtained when using COD 1 in the same way as PD 6493. COD 2 and COD 3 should be thought of as more accurate than COD 1 and they contain no factors of safety. To date, no proposals have been made about the use of material toughness data, but clearly a more elaborate plan is needed than that for COD 1.

In R6 Rev. 3, a number of fracture toughness parameters have been defined to provide an unambiguous means of interpreting fracture toughness data for use in an engineering assessment (4). The definitions are consistent with current national standards, but go beyond these taking account of current levels of understanding in fracture (26) and the recently proposed J test procedure of Neale et al (27). The parameters obtained are used to specify three different categories of analysis (4): category 1 to initiation of cracking, category 2 to a level of toughness enhanced by a small amount of ductile tearing where it is available, and category 3 to the complete resistance curve allowing a full instability analysis to be performed. By taking account of appropriate validity criteria using demonstrably conservative data and specific factors for the category 2 analysis, this allows limiting loading conditions to be determined up to which the specified event (initiation, instability, etc.) can be expected not to occur. Thus the analysis may be tailored to any specific requirements. For example, under normal operating loads it may be inappropriate to analyse beyond initiation, while for low probability fault conditions large amounts of tearing may be permitted.

A difficulty with all analysis techniques is how to establish what level of toughness to use. Statistical analysis, especially of widely scattered data, is seldom of help. For a steel which undergoes a ductile brittle transition there is often a specimen size effect (28, 29) and the available quantity of material is generally too little to evaluate

TABLE 3 - Comparison of treatment adopted for ^{S} stresses

Method	Equations
GE	$J_c = \frac{K^2\left((\sigma^P+\sigma^S), a_e\right)}{E'} + \alpha \xi_0 \sigma_0 c h_1 \left(\frac{P}{P_0}\right)^{n+1}$
EnJ	$J_c = \left(J_P^{\gamma} + J_{S(thermal)}^{\gamma} + J_{S(residual)}^{\gamma} \right)^{1/\gamma}$
R6 Rev. 3	$J_c = \left\{ \frac{K^P + K^S}{\left\{ \frac{E\varepsilon_{ref}}{L_r \sigma_y} + \frac{L_r^3 \sigma_y}{E \varepsilon_{ref}} \right\}^{-1/2} - \rho} \right\}^2 \frac{1}{E'}$
COD 3	$J_c = \frac{m}{E}\left\{ \sigma^P \sqrt{\pi a} \left(\frac{a_e}{a} + \frac{E\varepsilon_{ref}}{\sigma_{ref}} - 1 \right)^{1/2} + \sigma^S \sqrt{\pi a} \right\}^2$
COD 2	$J_c = \frac{m}{E}\left\{ \sigma^P \sqrt{\pi a} \frac{\sigma_y}{\sigma_n} \left[\frac{8}{\pi^2} \ln \sec \left(\frac{\pi}{2} \frac{\sigma_n}{\sigma_y} \right) \right]^{1/2} + \sigma^S \sqrt{\pi a} \right\}^2$
COD1	$J_c = \frac{2m}{E}\left\{ (\sigma^P + \sigma^S) \sqrt{\pi a} \right\}^2 ; \ \sigma_{nom} \leqslant 0.5$ $J_c = \frac{2m}{E}\left\{ \frac{\sigma^P + \sigma^S}{\sigma_y} - 0.25 \right\} \sigma_y^2 \pi a ; \ \sigma_{nom} > 0.5$

for this. Other problems also exist, in ensuring that the appropriate material is sampled by the crack tip, in judging whether heat affected zones should be tested, or in deciding whether pop-in events are significant. Up until now these problems have not been adequately addressed and the guidance which is given to overcome them comes from judgement rather than quantitative analysis. For this reason the R6 techniques require a study of the sensitivity of the result to variations in the toughness parameters before the necessary factors of safety are set. This area of establishing the appropriate fracture toughness values is one of the few relatively underdeveloped areas remaining in fracture mechanics.

TREATMENT OF THERMAL/RESIDUAL STRESSES

There are some occasions when these are sufficiently long range that they may act as mechanical stresses and in such cases they must be treated as such. In other cases they are self equilibrating, acting as secondary stresses, and these are termed ^{s} stresses. This class of stress must be treated differently from the mechanical (σ^{p}) stresses.

In all the COD procedures σ^{s} stresses are included in the equations as a simple addition, Table 1, separate from the elastic plastic correction term. This acknowledges the fact that σ^{s} stresses cannot cause failure under fully plastic conditions (30, 5) but makes no allowance for smaller scale plasticity effects which may arise, or for the interactive plasticity effects between the σ^{p} and σ^{s} stress fields. Such interactive effects depend upon the order of loading and can only be realistically evaluated by a detailed finite element analysis of the developing stress and strain fields local to the crack as it is being loaded. Nevertheless, simplified techniques can be developed which will produce a satisfactorily pessimistic method of analysis suitable for use in most practical cases. Highly complex cases can be treated by specialised methods (31, 32, 33).

The methods of incorporating σ^{s} stresses into the various analyses are sufficiently different to make direct comparison misleading, other than at an implied critical condition, J_c. This comparison is made in Table 3. In the GE scheme (8) the σ^{s} stresses appear only in the first order plastic term with the correction evaluated under the combined

loading, as required. This is also true of R6 Rev. 3, but in this case the combined plasticity effects are derived separately by virtue of the ρ parameter (Table 3). This parameter is a function of L_r and decreases to zero at $L_r > 1.05$ thus eliminating plasticity effects of σ^s at high net section stresses. In the EnJ method J_s is evaluated for the σ^s stresses using the standard EnJ equations (Table 1) and the necessary value of $\varepsilon_f/\varepsilon_y$ under the σ^s loading; this is then added to J_p, evaluated similarly for the σ^p loads, in the manner shown in the equation in Table 3. The term γ takes the value $0.5 + (\sigma^s + \sigma^p)/2\sigma_y$ up to a maximum value of 1. (10). This method is unique in aiming to satisfy all the requirements of σ^s analysis, while taking into account stress relaxation effects at high peak stresses and strain and displacement control effects, via the calculation of $\varepsilon_f/\varepsilon_y$ (as implied by the rising curve at $L_r > 1.2$ in Fig. 4). Difficulties abound, however, especially in what value to assign to cbsε. More discussion and guidance is needed on this before it can be considered a useful method. Moreover, the validity of applying the EnJ equations at $\varepsilon_f/\varepsilon_y > 1.2$ is not so self evident as the validity of the methods used in the GE and R6 Rev. 3 procedures, and the reasons for the method of adding J_p and J_s is also obscure.

VALIDATION

All the four techniques are simple ones, and as such cannot be expected to provide accurate descriptions of the true structural behaviour when all the complicating factors and uncertain parameters present in a real structure are taken into consideration. Good agreement between predictions and test results although praiseworthy, depends more upon good luck than good judgement and should not be regarded as the sole criterion of validity. Validation must also be addressed from the viewpoint of a satisfactory demonstration that the procedures can reliably achieve their intended objectives.

The GE scheme was derived to produce estimates of J applied. These were based upon results obtained using finite element methods so, not surprising, the results are consistent with these (6, 7). This consistency does not imply validity, however. For this the J estimates need to be compared with results obtained from structural tests. Unfortunately, such comparisons are confined to simple 2-dimensional test specimen geometries by the authors (6, 7, 8).

Attempts to validate the procedures by others has met with varying success.

In particular a test on a centre cracked panel of carbon-manganese steel was shown to be badly represented by Rousselier (21). As far as pressure vessels are concerned there has been no published attempt by the authors to validate the procedures but one attempt was made by a non-author to give a blind prediction for phase II of the EGF round robin exercise (22). This resulted in the expected underestimates because of the pessimistic representation of the crack geometry. It is clear that the results are highly sensitive to a number of features, especially the way the materials stress strain curve is represented and how closely the geometry in question may be represented by the 2-dimensional GE model.

The other technique which is aimed primarily at providing an estimate of J applied is EnJ. This technique was derived as an upper bound to a number of finite element J solutions obtained for a variety of geometries containing short cracks. Its extension to geometries with deep cracks may be made via the term $\varepsilon_f/\varepsilon_y$ (through cbsε) and this has been shown to be satisfactory in the case of some deep notched tension results (9). Such validation is severely limited, however, and is restricted to calculations by the author. Blind predictions have been made of compact tension specimens and pressure vessel tests in the EGF predictive exercises (19, 22) and these have proved to be generally satisfactory. Like the GE scheme, the results are sensitive to a crucial calculation, that of $\varepsilon_f/\varepsilon_y$, which contains corrections for both strain hardening and geometric effects, and the success of the procedure depends critically on the calculation of this quantity.

R6 Rev. 3 should be considered as a total package whose objective is to define conditions under which failure can be guaranteed to be avoided. Initially simple test specimen goemetries were used to demonstrate that the form of the basic equation (Table 1) was applicable to different geometries and crack sizes for materials as widely different as austenitic steel (16) and carbon-manganese steels (23, 34). This was done by comparing failure assessment diagrams derived both experimentally and from finite element methods with the R6 Rev. 3 equation (Table 1). The ability of the procedures to achieve their stated objective (i.e. avoid failure) was then demonstrated by applying

TABLE 4 - Validation of R6 Rev. 3

Test	Loading	Measured Quantities	R6 Rev. 3 Limiting Loads
PV test (EGFII A533B	pressure only	Max. pressure 80.5MPa	72.5MPa
PV test (EGFIV) SA weld	pressure +resid.	initiation pressure 60MPa	44.8MPa
PV test (HSST V8A) SA weld	pressure only	max. pressure 140MPa	120MPa
Pipe test (Batelle) austenitic steel	bending moment	initiation pressure 299KN max. pressure 443KN	253KN 363KN

the total procedures to a series of real structures which had been tested to failure, and for which adequate and relatively unambiguous data was available (4). These tests included pressure vessel test V8A in the US NRC Heavy Section steel Technology (HSST) programme (35), pressure vessel tests 1 and 3 in a CEGB test programme which were used in the EGF predictive exercise (22, 36) and a bend test on an austenitic pipe performed in the US NRC degraded pipework programme (37). The analysis details are contained in the R6 validation document (38) and the results are summarised in Table 4.

R6 has also been used both by authors and non-authors, to make blind predictions in the EGF predictive exercises and also for the HSST test V8A. In most cases the analysis was done using the original R6 curve (17) but in many instances the Rev. 3 equation was used. In no case were the procedures followed in detail, since a best estimate analysis was needed, so there was inevitably an element of variation to the results. However, on balance the predictions were in good agreement with the test results and the variation from user to user was not large (19, 22, 35, 36).

This experimental validation covers the application of mechanical loads to cracked structures both in the absence of residual stresses and in their presence. It does not cover situations where thermal stresses exist. However, these would not be expected to behave differently in principle to residual stresses. The loading sequence has an effect on the development of plasticity from a crack, and hence on the magnitude of the applied J (39). The procedures for thermal and residual stresses recommended in R6 Rev. 3 have been compared with a number of finite element results obtained using different loading sequences and have been shown to be broadly pessimistic (33). There are situations where a non-pessimistic result is potentially possible, and these are highlighted in the status notes to the document (3).

Validation of all 3 COD tiers is not comprehensive at present, mainly because of the developing status of COD 2 and COD 3. For example, there is only one recorded validity test for COD 3 (5). Nevertheless, since COD 3 is so similar to R6 Rev. 3 for mechanical loading, the R6 validation would be expected to serve COD 3 also. However, this depends upon

how the material toughness data is treated in COD 3 and upon the value of m (Table 2). The treatment of σ^S stresses in COD 3 is not validated by the R6 Rev. 3 results and this should be treated with caution, especially in view of the load sequence effect (39).

Where COD 3 is shown to be valid, the COD 2 must also be so. COD 1 is different, however, in its regime of application, in its use of materials toughness data, and in its use of factors. Nevertheless because of its similarity to the original COD procedure (18, 24) the validation for that procedure should be equally applicable to COD 1. This showed that for a series of wide plate tests the lowest value of COD obtained in 3 (relevant) standard COD tests underestimated the failure load 97% of the time (25). The wide plate tests included tests on non-stress relieved welded joints, and these were also satisfactory provided that the level of residual stress was assumed to be uniformly equal to the yield stress. Although of all validity tests this is the only one with an element of statistical significance, its empirical nature and simple wide plate test basis must compromise its credibility. However, it should not be forgotten that the COD technique in BSI PD 6493 (24) has been widely used for plant applications and that there is no record of any service failure occurring subsequently.

SUMMARY OF KEY POINTS

GE Scheme

Advantages: capable of accurate estimate of J applied for 2-dimensional and axisymmetric geometries, has facility to evaluate under fixed displacements; provides for potential interaction between σ^S and σ^P stresses in small scale yielding regime.

Disadvantages: available solutions are limited to few 2-dimensional geometries, so not generally applicable; representation of material's tensile data is unsatisfactory and user sensitive; validation is limited to comparison between finite element solutions and test results on simple geometries; no guidance is given on use of material's toughness data; over pessimistic for peak σ^S stresses above yield; does not provide independent safeguard to avoid plastic collapse.

On balance, although capable of high accuracy in some limited instances the results are highly user sensitive so the validity of each analysis must be judged separately. The scheme needs further development before it can be relied on for general application.

R6 Rev. 3

Advantages: objective of analysis is clear in that techniques provide a total package biased in such a way that failure is avoided; uses best possible means of representing tensile properties; defines appropriate material toughness properties unambiguously; validation is the most extensive (of the four methods) based upon finite element analysis, test specimen results and structural test results; applicable to all geometries with facility for developing empirical solutions where appropriate; interaction between σ^p and σ^s stresses provided for; user judgement required to be rationally justified; plastic limit analysis automatically incorporated.

Disadvantages: assumes mechanical loads are load controlled, cannot evaluate under fixed displacements; over pessimistic for very high peak σ^s stresses.

On balance, the procedures provide solutions which are relatively consistent. Where user judgement is needed it is not hidden. It is of general applicability, its lack of dependence on finite element analysis and user idiosyneracies makes it generally reliable without the need for continuous validation.

EnJ

Advantages: capable of allowing for fixed displacement loadings; capable of analysing under conditions of peak σ^s stresses greater than yield; is not restricted to simple geometries; safeguards against plastic collapse by independent analysis.

Disadvantages: procedure is still evolving and is not explicitly enumerated in any single publication; crucial step in analysis is calculation of $\varepsilon_f/\varepsilon_y$ and guidance for this is inadequate; validation is extremely limited, especially in respect of fixed displacement regime; form of analysis is incompatible with other procedures based on load control, and therefore suspect here; reason for

many of the recommendations are obscure; tensile data is unrealistically represented; no guidance on material toughness data.

On balance, this very useful concept is marred by inadequate guidance on how to calculate the crucial parameter $\varepsilon_f/\varepsilon_y$, and by the lack of validation. It is likely to be most useful in situations where σ^s stresses dominate, or where the loading system is displacement controlled. It is not yet well enough developed to be generally applicable.

COD techniques

Advantages: COD 1 is easy to use and generally applicable at low net section stress levels, unambiguous in use of material toughness data, well defined with clear objectives, apparently well validated on wide plate specimens; COD 3 has advantages of functional form of R6 Rev. 3; COD 2 is good approximation to COD 3 where no advantage is taken of work hardening; both COD 2 and COD 3 are generally applicable.

Disadvantages: COD 2 and COD 3 are still under development. At present the disadvantages are: treatment of σ^s stresses makes no allowance for interaction with σ^p stresses in small scale yielding; no guidance given on use of material toughness data; no facility for treating displacement controlled loading; explicit validation is poor (although may be inferred from R6 Rev. 3 validation); no guidance on judgement of results; COD 3 contains no safeguard against plastic collapse.

On balance, the COD techniques have the potential to be as generally and unambiguously applicable as R6 Rev. 3 when fully developed. More consideration needs to be given to the combined effects of σ^p and σ^s stresses, especially since theoretical arguments and finite element solutions indicate interaction may be significant in the small scale yielding regime.

CONCLUDING COMMENT

It should be recognised by the potential user that the different methods of analysis are tailored to different types of problem, and that no simple solution can be universally excellent. The user should choose his method from a knowledge of the type of structure he is analysing, the loading systems, the available material property data and the type of result he

is looking for, taking into account the uncertainties in the data base and how these may be turned to advantage.

This paper was intended not to list the competing advantages and disadvantages of the various procedures, so much as to illustrate their strengths and weaknesses, to show where they have similar features and to highlight areas where further development is needed. There are many such areas, but two of these may be identified as having the most immediate potential benefit. The first is in the treatment fracture toughness data, especially when this is highly scattered. It is easy for the purist to insist on large sizes and numbers of specimens, but this freedom is rarely available in practice. The second is in the analysis of σ^s stresses, especially where local peaks exceed the elastic limit and high local strains are obtained.

ACKNOWLEDGEMENTS

The work was done at the Central Electricity Research Laboratories of the Technology Planning and Research Division of the C.E.G.B. and is published by permission of the Central Electricity Research Laboratories.

REFERENCES

(1) Rice, J. R., Trans. ASME, J of Applied Mechanics, Vol. 35 1968, p. 379-386.

(2) Hutchinson, J. W. and Paris, P. C., Stability analysis of J-controlled crack growth, ASTM STP 668, 1979 p. 37.

(3) Milne, I., Ainsworth, R. A., Dowling, A. R. and Stewart, A. T., Assessment of the integrity of structures containing defects. CEGB report R/H/R6 - Rev. 3 (1986).

(4) Ainsworth, R. A., Dowling, A. R., Milne, I. and Stewart, A. T., Revision 3 of R6, its background and validity, proc. Int. Conf. on Fracture Control of Engineering Structures, ECF 6, paper nr 151 1986.

(5) Anderson, T. L., Leggatt, R. H., and Garwood, S. J. in proc. of Workshop on CTOD Methodology, GKSS, Geesthacht, Germany 1985.

(6) Kumar, V., German, M. D., and Shih, C. F., Estimation technique for the prediction of elastic plastic fracture of structural components of nuclear systems. General Electric Co. report SRD-80-094 Schenectady, N.Y. 1980.

(7) Kumar, V., German, M. D. and Shih, C. F., An engineering approach to elastic plastic fracture analysis. EPRI report NP 1931 1981.

(8) Kumar, V., German, M. D., Wilkening, W. W., Andrews, W. R., de Lorenzi, H. G. and Mowbray, D. F., Advances in elastic plastic fracture analysis, EPRI report NP 3607, 1984.

(9) Turner, C. E., Further developments of a J-based design curve, ASTM STP 803, 1983 p. II80-II102.

(10) Turner, C. E., A J-based fracture safe estimation procedure, EnJ in proc. of 4th Advanced seminar on fracture mechanics, Joint Research Centre, Ispra, Italy, p. 397-410, 1983.

(11) Bloom, J. M. in proc. of Ductile Fracture Public Meeting, EPRI, Palo Alto, Calif. 1980.

(12) Paris, P. C. and Johnson, R. E., A method of application of elastic plastic fracture mechanics to nuclear vessel analysis, in ASTM STP 803, p. II5-II40, 1983.

(13) Ainsworth, R. A. in Eng. Fracture Mechanics, vol. 19 1984 p. 633.

(14) Milne, I., Int. J of Press. Vess. & Piping Vol. 13 p. 107-125, 1983.

(15) Ainsworth, R. A., Chell, G. G. and Milne, I., proc. of CSNI/NRC Ductile piping fracture mechanics workshop, San Antonio, Texas 1984.

(16) Akhurst, K. N. and Milne, I., Int. Conf. on Application of Fracture Mechanics to Materials and Structures, Freiburg 1983.

(17) Harrison, P. R., Loosemore, K. and Milne, I., Assessment of the integrity of structures containing defects, CEGB report R/H/R6, 1976.

(18) Burdekin, F. M. and Dawes, M. G., proc. of conf. on Application of fracture mechanics to pressure vessel technology, Inst. Mech. Eng., London, 1971.

(19) Milne, I., Report on EGF task group 1 exercise in predicting ductile instability, phase I compact tension specimens, to be published.

(20) Marandet B., and de Roo, P., in IRSID report RE 895, March 1982.

(21) Rousselier, G. in proc. of 4th Advanced Seminar on Fracture Mechanics, Joint Research Centre, Ispra, Italy 1983 p. 313-396.

(22) Milne, I and Knee, N., Report on EGF Task group 1 exercised in predicting ductile instability: phase II experimental cracked pressure vessel. CEGB report TPRD/L/2771/N84, 1985.

(23) Gates, R. S., Gladwin, D. N., Bradford, R. and Green, G., Effects of geometry on failure assessment diagrams for C-Mn steels: a comparison of CCP and CT geometries. CEGB report SWR/SSD/0622/N/85 1986.

(24) British Standards Institution. Guidance on some methods for the derivation of acceptance levels for defects in fusion welded joints, B.S. PD6493 March 1980.

(25) Kamath, M. S., The COD design curve: an assessment of validity using wide plate tests. Welding Institute report 71/1978/E, September 1979.

(26) Milne, I. and Curry, D. A. in ASTM STP 803, 1983 p. II 278-II290.

(27) Neale, B. K., Curry, D. A., Green, G., Haigh, J. R. and Akhurst, K. N., A procedure for the determination of the fracture resistance of ductile steels, CEGB report TPRD/B/0496/N84 1984.

(28) Milne, I. and Chell, G. G., in ASTM STP 668 1979 p. 358-377.

(29) Landes, J. D. and Schaffer, D. H. in ASTM STP 700 1980.

(30) Chell, G. G. and Ewing, D. J. F. in Int. J. of Fracture Vol. 13, 1977, p. 467.

(31) Ainsworth, R. A., Neale, B. K. and Price, H. in proc. of Conf. on tolerance of flaws in pressurised components, Inst. Mech. Eng. London, 1978.

(32) Chell, G. G., A J estimation procedure for combined mechanical thermal and residual stresses, CEGB report TPRD/L/2930/N85 1985.

(33) Blackburn, W. S. Assessment of cracks under secondary and combined loading CEGB report TPRD/B/0447/N84 1984.

(34) Green, G., Gladwin, D. N., Bradford, R and Stewart, A. T., Strain hardening failure assessment diagrams derived from C-Mn steel compact tension specimens: implications of the experimental and analytical results, CEGB report SWR/SSD/0491/N/84, 1984.

(35) Bryan, B. H., Bass, B. R., Bryson, J. W. and Merkle, J. G. in Light Water Reactor Structural Integrity ed. by K. E. Stahlkopf and L. E. Steele, 1984, p. 175-210.

(36) Knee, N., Experimental results and analytical predictions for failure in a weld repaired test pressure vessel (EGF phase IV) to be publisted.

(37) Wilkowski, G. M., Ahmed J., Barnes, C. R., Broek, D., Kramer, G., Landon, M., Marschall, C. W., Maxey, W., Nakagaki, M., Scott, P., Papaspyropoulos, V., Pasupathi, V. and Popelar, C., Degraded piping program - phase II Vol. 2, NUREG/CR-4082 1985.

(38) Milne, I., Ainsworth, R. A., Dowling, A. R. and Stewart, A. T., Assessment of the integrity of structures containing defects: validation. CEGB report to be published 1986.

(39) Hellen, T. K. and Blackburn, W. S., Post yield fracture mechanics analysis of the combined thermal and mechanical loading of a centre cracked plate. CEGB report TPRD/B/0613/R85, 1985.

SYMBOLS AND DEFINITIONS

a	=	crack depth
a_e	=	effective crack depth
α	=	Ramberg-Osgood parameter
β_t	=	$0.8\,\sigma_t/\sigma$ (10)
β_b	=	$1.2\,(1-a/t)\,\sigma_b/\sigma$ (10)
c	=	t-a (6,7,8)
δ, δ_{crit}	=	crack tip opening displacement (critical), COD
E	=	Youngs modulus, $E^1 = E/(1-\nu^2)$ for plane strain
ε	=	strain
$\varepsilon_{ref}, \varepsilon_o, \varepsilon_y$	=	reference strain-general, specific (6), yield
$\varepsilon_f/\varepsilon_y$	=	effective strain ratio (10)
G_y	=	strain energy release rate, at applied yield stress (10)
g	=	geometry factor (10)
h	=	hardening factor = 1/N+1 (10)
h_1	=	hardening and geometry term, h_1 (a/t,n) (6,7,8)
J	=	Elastic-plastic parameter characterising crack tip loading
J_p, J_s	=	J for σ^p loading, J for σ^s loading
K	=	Linear elastic parameter characterising crack tip loading
K^p, K^s	=	K for σ^p loading, K for σ^s loading
ℓ	=	crack length
L_r	=	Load/(local) yield load; σ_n/σ_y (3,4,5)

m	=	factor between J and COD, m = $J/\sigma_y\delta$
N	=	strain hardening index (10)
n	=	Ramberg-Osgood strain hardening index (6,7,8)
P	=	load
P_o	=	reference load, sometimes equal to yield load (6, 7, 8)
$\sigma, \sigma^t, \sigma^s$	=	applied stress (mechanical) (thermal or residual)
σ_b, σ_t	=	bending stress, tensile stress (9,10)
$\sigma_{ref}, \sigma_o, \sigma_y$	=	reference stress-general, specific (6), yield
σ_n	=	net section stress
t	=	section thickness
Y	=	Linear elastic K calibration factor
ν	=	Poisson's ratio

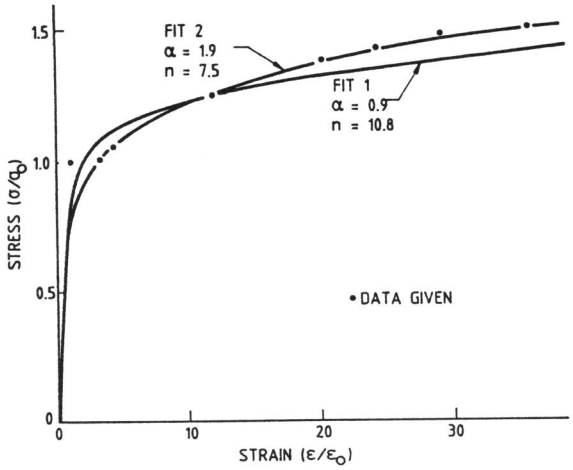

Fig. 1 Stress-strain data and R.O. laws

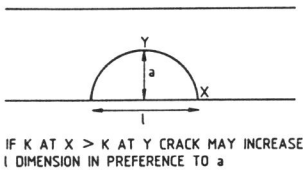

Fig. 2 Potential crack growth directions

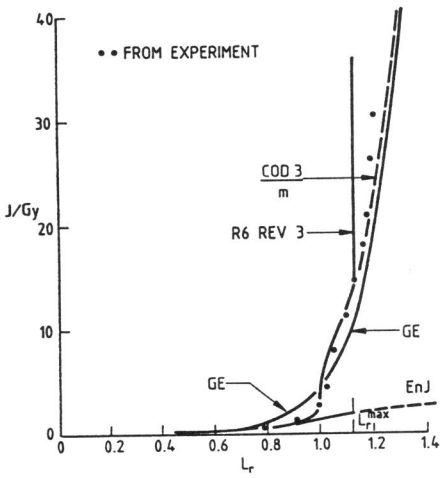

Fig. 3 Comparison of methods with test results

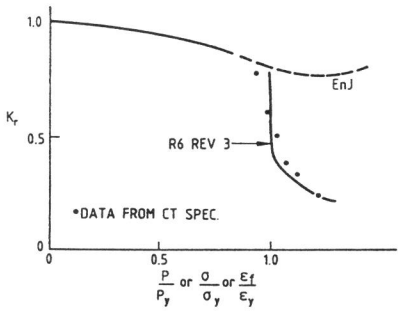

Fig. 4 R6 Rev.3, EnJ and test data from CT spec.

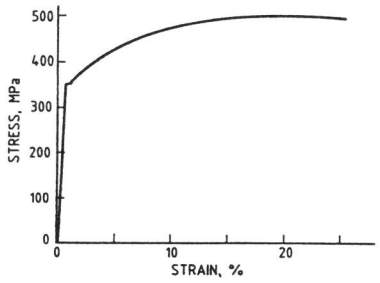

Fig. 5 Tensile data for C-Mn steel

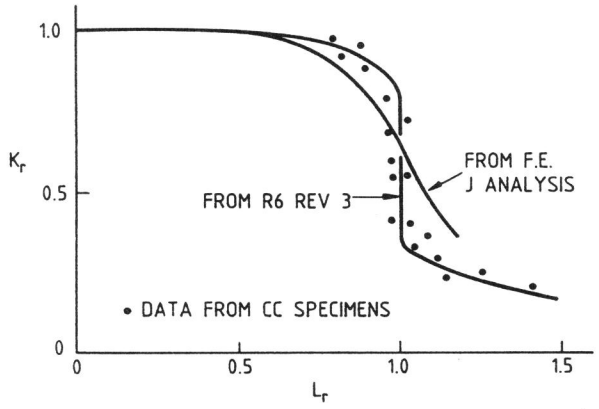

Fig. 6 FADs for C-Mn steel and tensile test results